Journal of Physics and Chemistry of Solids 111 (2017) 403–409

Contents lists available at ScienceDirect

Journal of Physics and Chemistry of Solids

journal homepage: www.elsevier.com/locate/jpcs

First-principles investigation on the structural, elastic and electronic properties and mechanism on the photocatalytic properties for $SrNbO_3$ and $Sr_{0.97}NbO_3$

Yong-Qiang Xu [a,b,*], Shao-Yi Wu [a,**], Jia-Xing Guo [a], Li-Na Wu [a], Li Peng [a]

[a] Department of Applied Physics, School of Physical Electronics, University of Electronic Science and Technology of China, Chengdu 610054, PR China
[b] College of Physics and Electronic Information, Gannan Normal University, Ganzhou 341000, PR China

ARTICLE INFO

Keywords:
Electronic structures
Photocatalytic properties
Elasticity
First-principles
$SrNbO_3$

ABSTRACT

The structural, elastic and electronic properties of perfect $SrNbO_3$ and defective $Sr_{0.97}NbO_3$ are investigated by employing the plane-wave pseudopotentials methods based on density functional theory (DFT). The photocatalytic activity is also discussed for both systems based on the obtained electronic structures. The single-crystal elastic constants, polycrystalline elastic modulus, Poisson's ratio and anisotropy factors are obtained from the Voigt-Reuss-Hill approximations. Further, the elastic anisotropy is discussed and visualized in the light of the elastic properties. The direction dependence of Young's modulus is also compared for the two systems. The Fermi levels going through the conduction bands indicate metallic nature of $SrNbO_3$ and $Sr_{0.97}NbO_3$. The transitions from CB to B band can yield visible light absorption. From the effects of the electronic and crystallographic structures on photocatalytic activity, perfect $SrNbO_3$ can show higher photocatalytic activity than defective $Sr_{0.97}NbO_3$. The related physical properties of defective $Sr_{0.97}NbO_3$ are predicted for the first time. The present study would contribute to the further researches on the photocatalytic properties of $SrNbO_3$ based systems.

1. Introduction

With the emergence of photocatalytic techniques of visible light driven water splitting to produce hydrogen, great attention has been paid to visible light photocatalysts with ideal band gaps of about 2.0 eV for high efficient visible light absorption [1–4]. However, present popular semiconductor photocatalysts such as TiO_2, ZnO, $NaNbO_3$, $KNbO_3$, $NaTaO_3$ and $KTaO_3$ have larger band gaps than 2.0 eV [5–10]. So their band gaps need to be modulated to enhance visible light absorption, e.g., by means of metal or non-metal doping [5,6,11–21]. However, dopant-free photocatalytic materials are more attractive due to the practicability. Recently, $SrNbO_3$ crystal is found to be an effective visible light driven photocatalyst without doping [22]. Since then an increasing number of researches have been carried out to focus on its photocatalytic properties, e.g., the analysis of the photocatalytic mechanisms based on the first-principles calculations [23,24]. Additionally, some other unique physical properties have also been explored for strontium niobate based systems, involving low susceptibility [25], high electrical conductivity [26], high-temperature ferroelectricity [27], anisotropic electric transportation [28] and anisotropic thermoelectric properties [29], etc. Therefore, strontium niobate as a promising metallic oxide photocatalyst can afford promising applications in energy production and environmental remediation aspects, and its electronic structures and optical properties (especially visible light absorption) are worthy to be further investigated.

Experimentally, the stoichiometric $SrNbO_3$ phase with cubic perovskite structure is difficultly to be attained due to frequent Sr deficiencies in bulk samples [30]. The available experimental results about perfect $SrNbO_3$ are very limited so far [31,32]. On the contrary, a great number of Sr deficient Sr_xNbO_3 ($0.5 < x < 1$) structures have been synthesized [30–35]. In addition, some other compositions (e.g., $SrNbO_{3.4}$ and $SrNbO_{3.5}$) with higher oxygen contents than the stoichiometric phase have also been synthesized successively [36–39]. Admittedly, Sr defects will produce great influences on the structures and properties of $SrNbO_3$, particularly photocatalytic properties [23]. However, to the best of our knowledge, the physical properties relevant to the photocatalytic activity have not been clarified for this early $Sr_{0.97}NbO_3$ structure with low Sr defect concentration up to now, except its crystal structure was measured

* Corresponding author. Department of Applied Physics, School of Physical Electronics, University of Electronic Science and Technology of China, Chengdu 610054, PR China.
** Corresponding author.
E-mail addresses: yqxu666@163.com (Y.-Q. Xu), wushaoyi@uestc.edu.cn (S.-Y. Wu).

http://dx.doi.org/10.1016/j.jpcs.2017.08.030
Received 30 May 2017; Received in revised form 19 July 2017; Accepted 19 August 2017
Available online 23 August 2017

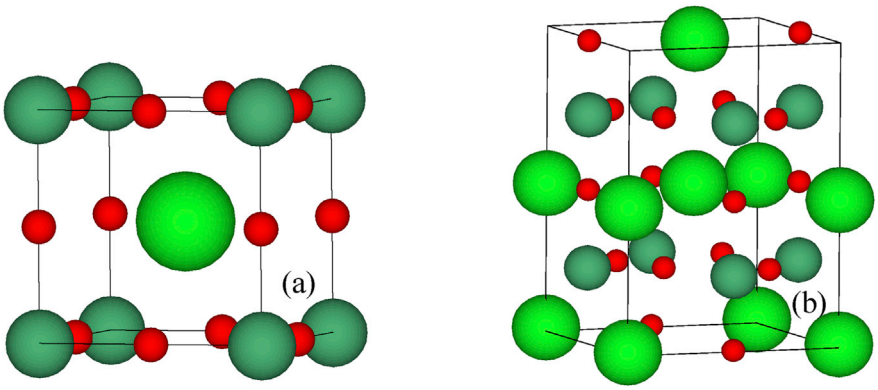

Fig. 1. A unit cell of perfect $SrNbO_3$ (a) and defective $Sr_{0.97}NbO_3$ (b).

Table 1
The calculated lattice parameters a_0 (in Å), equilibrium bulk modulus B_0 (in GPa) and pressure derivative $B'$of the bulk modulus for $SrNbO_3$ and $Sr_{0.97}NbO_3$ with LDA, PBE, PBEsol, and HSE06 schemes.

			a_0			B_0	B'
$SrNbO_3$	Present	LDA	4.019			196.71	4.333
		PBE	4.091			169.03	4.289
		PBEsol	4.052			182.58	4.426
		HSE06	4.052			188.77	4.367
	Theoretical	GGA	4.073[a]			173.46[a]	
		GW	4.03[b]				
		LDA	3.997[c]				
	Experimental		4.024[d], 4.023[e],	4.0285[f]			
			a	b	c	B_0	B'
$Sr_{0.97}NbO_3$	Present	LDA	5.6849	5.6789	8.0521	198.44	4.434
		PBE	5.7878	5.7817	8.1978	170.33	4.406
		PBEsol	5.7332	5.7272	8.1205	184.32	4.439
		HSE06	5.7274	5.7214	8.1123	190.39	4.394
	Experimental		5.6881[e]	5.6821[e]	8.0566[e]		

[a] Ref. [47].
[b] Ref. [24].
[c] Ref. [48].
[d] Ref. [31].
[e] Ref. [30].
[f] Ref. [32].

Table 2
Calculated elastic constants (in GPa) and mechanical properties parameters for $SrNbO_3$ and $Sr_{0.97}NbO_3$. (*B, G, E* (in GPa)).

$SrNbO_3$	C_{11}	C_{12}	C_{44}	A (A^U)	B	G	E	v	B/G
	364.05 282.45[a]	102.65 118.97[a]	57.98 56.75[a]	0.44 (0.84)	189.78 173.46[a]	80.82	212.33	0.31	2.35
$Sr_{0.97}NbO_3$	C_{11}	C_{12}	C_{13}	C_{22}	C_{23}	C_{33}	C_{44}	C_{55}	C_{66}
	280.56	164.26	92.19	287.48	93.59	367.67	59.61	58.09	144.14
	A_1	A_2	A_3	A^U	B	G	E	v	B/G
	0.51	0.50	2.41	0.94	181.72	84.15	218.70	0.30	2.15

[a] Ref. [47], in which these values were obtained with GGA scheme.

[30]. So the physical properties of $Sr_{0.97}NbO_3$ and its possibility of visible light photocatalytic ability need to be further studied. Meanwhile, the influences of the differences in structure and physical properties between stoichiometric $SrNbO_3$ and defective $Sr_{0.97}NbO_3$ crystals on photocatalytic efficiency deserve to be clarified. In addition, despite low Sr defect concentration, the symmetry of $Sr_{0.97}NbO_3$ crystal is reduced to orthorhombic, its mechanical and elastic properties may exhibit some novelty that are worthy to be further examined.

In order to shed light on these points, the elasticity, electronic structures and photocatalytic properties of perfect $SrNbO_3$ and defective $Sr_{0.97}NbO_3$ crystals are investigated and compared in the frame of first-principles density functional theory (DFT) in this work. The article is organized as follows. In Section 2, we give a brief description of the method of the calculations for the elasticity and electronic properties. The results and discussions are provided in Section 3. Conclusions are presented in Section 4.

2. Computational methods

The geometric structures of $SrNbO_3$ and $Sr_{0.97}NbO_3$ crystals are theoretically studied by means of first-principles calculations based on the local density approximation (LDA) [40], generalized gradient approximation (GGA) of Perdew-Burke-Ernzerhof (PBE) [41], revised Perdew-Burke-Ernzerhof generalized gradient approximation (PBEsol)